C. R. Physique 3 (2002) 301–317

Solides, fluides : propriétés électroniques et optiques/*Solids, fluids: electronic and optical properties*
(Solides, fluides : structure/*Solids, fluids: structure*)

DOSSIER

AGRÉGATS COMME PRÉCURSEURS DES NANO-OBJETS
CLUSTERS AS PRECURSORS OF NANO-OBJECTS

Structure of nano-objects through polarizability and dipole measurements

Michel Broyer, Rodolphe Antoine, Emmanuel Benichou, Isabelle Compagnon, Philippe Dugourd, Driss Rayane

Laboratoire de spectrométrie ionique et moléculaire UMR n 5579, CNRS et université Claude Bernard, Lyon I, bâtiment Alfred Kastler, 43, boulevard du 11 Novembre 1918, 69622 Villeurbanne cedex, France

Received 14 December 2001; accepted 7 January 2002

Note presented by Guy Laval.

Abstract The electric polarizability and the electric permanent dipole are important quantities for understanding the electronic properties of a cluster. Experimental techniques, the simulations necessary to interpret the experimental results, and a review of measurements on atomic and mixed clusters are presented. For atomic clusters, the polarizability is related to the type of bonding. In simple metal clusters such as alkali clusters, the results are well interpreted by the electron delocalization characteristic of the metallic bonding. In other metal clusters, the polarizability reflects the difficulty of establishing a clear and regular picture of the size evolution of electronic properties. The size evolution observed for covalent and semiconductor clusters is different from the evolution for metal clusters, and the influence of the geometry is preponderant, as demonstrated in the case of fullerenes. For mixed clusters, the measurements of the electric dipole allows one to deduce the charge transfers and the geometric arrangement. This is illustrated in the case of the metal-fullerene system and alkali halide clusters. ***To cite this article: M. Broyer et al., C. R. Physique 3 (2002) 301–317.*** © 2002 Académie des sciences/Éditions scientifiques et médicales Elsevier SAS

cluster / electric polarizability / electric permanent dipole / metal-fullerene system / alkali halide cluster

Structure des nano-objets determinée par mesures de polarisabilité et de dipôle

Résumé La polarisabilité statique et le dipôle électrique permanent sont des quantités importantes pour comprendre les propriétés électroniques et structurales d'un agrégat. Dans cet article nous présentons les différents montages expérimentaux utilisés pour ces mesures et les simulations nécessaires à l'interprétation des résultats. Les cas des agrégats polaires et non polaires sont distingués et l'influence de la rigidité de l'agrégat sur son mouvement dans un champ électrique est discutée. Ces deux premières parties sont suivies par une revue des mesures réalisées sur des agrégats atomiques et des agrégats mixtes. Pour les agrégats atomiques, la polarisabilité est reliée à la nature de la liaison. Dans les métaux simples comme les agrégats alcalins, les résultats sont bien expliqués par la délocalisation des électrons de valence, caractéristique de la liaison métallique. Pour les autres métaux,

E-mail address: Broyer@lasim.univ-lyon1.fr (M. Broyer).

S1631-0705(02)01318-X/FLA

la polarisabilité reflète la difficulté à décrire simplement les propriétés électroniques de ces agrégats. Dans le cas de l'aluminium, les mesures de polarisabilité mettent en évidence une transition non-métal–métal avec l'augmentation de la taille de l'agrégat. Dans le cas du nickel, de fortes variations avec la taille sont observées, certainement dues à un fort couplage entre propriétés électroniques et structure atomique. L'évolution avec la taille pour les agrégats semi-conducteurs (silicium, germanium) et covalents (fullerènes) est différente de celle observée pour les agrégats métalliques. Les mesures réalisées sur les fullerènes illustrent l'influence prépondérante de la géométrie sur la valeur de la polarisabilité. Dans le cas des agrégats mixtes, le dipôle électrique est la mesure la plus simple de la densité de charge dans l'agrégat. Ce dipôle dépend des transferts de charge et de l'arrangement géométrique des atomes dans la particule. Les mesures de dipôle électrique permanent sont illustrées par les résultats obtenus récemment sur deux exemples très différents : les agrégats mixtes métal-fullerène où un fort transfert de charge se produit et les agrégats d'halogénure d'alcalin dominés par une structure ionique. ***Pour citer cet article : M. Broyer et al., C. R. Physique 3 (2002) 301–317.*** © 2002 Académie des sciences/Éditions scientifiques et médicales Elsevier SAS

agrégat / polarisabilité statique / dipôle électrique permanent / métal-fullerène / agrégats d'halogénure d'alcalin

1. Introduction

The miniaturization of electronic devices and the advent of nanotechnology render it essential to understand the properties of atomic clusters. On the same point of view, the study of mixed clusters constituted of materials having different electronic properties is crucial in designing complex nanostructures made of small different nanoparticules and to take into account the charge transfers occurring in nanocontacts. The geometric and electronic structures of small clusters, having typically ten to several hundred atoms, may be investigated by various techniques [1] and references therein, such as laser spectroscopy, including ionization potentials measurements and optical properties [1–3], photoelectron spectroscopy [3,4] and imaging [5], photofragmentation, unimolecular evaporation [6,7] and ion mobility [8]. Electronic properties are mainly deduced from spectroscopy experiments which measured transitions between different electronic states or different charge states of the clusters. This tends to complicate the interpretation of the experiments. It is not always easy to determine the ground state properties which are the most essential for applications in nanoelectronics, and also to test the theoretical methods and calculations of the studied clusters. In this respect, the direct measurement of the electric polarizability is a direct probe of the cluster ground state and consequently of both geometric and electronic properties. In the same way the measurement of the permanent dipole of mixed clusters is one of the best methods to investigate charge transfers and geometric arrangements of these complex systems.

Electric polarizability and dipole may be in principle easily measured in beam deviation experiments in a static electric field gradient [9,10]. For clusters, the first experiment was performed by Knight et al. [11] on sodium and potassium clusters. Other measurements have been then performed on alkali clusters including lithium and mixed lithium sodium clusters [12] aluminum clusters [13], semiconductor clusters [14] and insulating clusters such as C_{60} and C_{70} clusters [15,16]. Recently Bonin et al. [17] have measured the optical polarizability of C_{60} in performing the beam deviation by the standing wave of a Nd^{3+}YAG laser ($\lambda = 1.064$ μm). This last method is quite complementary, it has the advantage of using a different experimental scheme and of providing a.c. polarizability.

Electric dipoles may be also deduced from deviation measurements. However, as explained in the following, the resulting beam profile depends strongly whether the cluster is rigid or not. The same situation is encountered in magnetic clusters [18–21] for the susceptibility measured in beam deviation by a magnetic field gradient. However, we expect that the coupling between electric dipole and vibrational motion is easier

to interpret and model [22,23]. Finally, the temperature dependence of the intrinsic polarizability of alkali clusters was investigated theoretically [24–27] and recent measurements [28] shows that the polarizability may be dependent on beam conditions.

In the present paper, we give an overview of recent results on electric dipole and polarizability of atomic clusters and mixed clusters. The paper is divided in six parts. After the introduction, the second part is devoted to the experimental techniques, in the third part, we present the simulations necessary to extract permanent dipole and intrinsic polarizability from the experiment. In the fourth part, the results on atomic clusters are given and discussed. In the fifth part mixed clusters with strong charge transfers are investigated, these systems being specially interesting with respect to permanent dipole and electric susceptibility. Finally, we end with a brief conclusion.

2. Experimental techniques

Static polarizability measurements are performed by deflecting a well-collimated beam through a static inhomogeneous transverse electric field. All the experiments using static fields are similar [11,13,14,28–30]. We describe here, as an example, the apparatus used in our laboratory (Fig. 1). The experiment consists in a laser vaporization source coupled to an electric deflector and a mass spectrometer. The clusters are produced in a simple or double rod laser vaporization source (the second or third harmonics of a Nd^{3+} : YAG laser are used for the laser ablation) and are entrained by a inert gas pulse. They leave the source through a 5 cm long nozzle which temperature can be adjusted from 80 K to 500 K. After two skimmers, the beam is collimated by two rectangular slits (0.4 mm width) and travels through the electric deflector ('two-wires' electric field configuration). The electric field and its gradient in the deflector are $F = 1.63 \times 10^7$ Vm^{-1} and $\nabla F = 2.82 \times 10^9$ Vm^{-2} respectively, for a voltage of 27 kV across the two poles. Clusters are ionized one meter after the deflector in the extraction region of a position sensitive time of flight mass spectrometer. The mass of the cluster and the profile of the beam are obtained from the arrival time at the detector [10]. The beam profile is measured as a function of the electric field in the deflector. A mechanical chopper located in front of the first slit allows us to select and measure the velocity v of the beam.

In the deflector, a cluster is subjected to an instantaneous force:

$$\vec{f} = \vec{\mu} \nabla \vec{F} \tag{1}$$

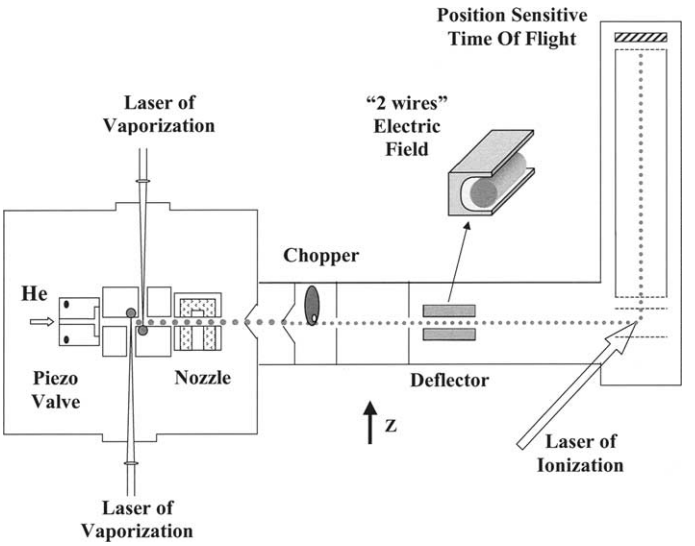

Figure 1. Schematic of an experimental setup for electric beam deflection experiments.

where $\vec{\mu}$ is the electric dipole of the cluster in the field. The deviation d for a cluster of mass m with a velocity v given by:

$$d = \frac{K\langle f\rangle}{mv^2} \tag{2}$$

where K is a geometric factor. This electric field leads to a broadening or/and a global deviation of the cluster beam.

3. Simulations

In a static electric field $\vec{F}$, the dipole moment of a particle is given by:

$$\vec{\mu} = \vec{\mu}_0 + \overleftrightarrow{\alpha}\vec{F} + \cdots \tag{3}$$

$\vec{\mu}_0$ is the permanent dipole of the particle and $\overleftrightarrow{\alpha}$ is the tensor of polarizability. Additional terms in the development can be neglected for the values of the field and of the gradient of the field that are used in static electric field experiments (see, for example, [31] for a discussion of additional terms). In the deviator, the average force is:

$$\langle f\rangle = \langle \mu_Z\rangle \nabla F_Z = \left\langle \left(\vec{\mu}_0 + \overleftrightarrow{\alpha}\vec{F}\right)\cdot\vec{Z}\right\rangle \nabla F_Z \tag{4}$$

where Z is the direction of the electric field. To simulate the deviation of the beam it is necessary to compute the average value of the projection of the cluster dipole on the axis of the electric field. We will first discuss nonpolar clusters (for example metal clusters, silicon clusters, ...) then we will discuss polar clusters (ionic clusters, metal carbon clusters, ...).

3.1. Nonpolar clusters

For nonpolar clusters, the only contribution to the dipole is coming from the electronic polarizability (second term in the right-hand of Eq. (3)). The induced dipole is proportional to the value of the electric field. For a spherical cluster it is simply given by $\mu_Z = \alpha F_Z$ where α is the polarizability of the cluster on any axis. For nonspherical clusters, the second order rank tensor of polarizability is not scalar. However, the rotational average value of the 'anisotropic part' of the polarizability $(\overleftrightarrow{\alpha} - \frac{1}{3}\mathrm{Tr}(\overleftrightarrow{\alpha})\overleftrightarrow{I})$ is small and it is a very good approximation to use:

$$\mu_Z \approx \alpha_{\mathrm{avg}} F_Z \quad \text{with} \quad \alpha_{\mathrm{avg}} = \frac{1}{3}\mathrm{Tr}(\overleftrightarrow{\alpha}) \tag{5}$$

A full treatment of the asymmetric part of the polarizability for linear molecules can be found in references [32,33]. The deviation of a nonpolar cluster obtained from Eqs. (2) and (5) is:

$$d = K\frac{\alpha F \nabla F}{mv^2} \tag{6}$$

The electric field induces a global shift d of the molecular beam toward the high electric field region. This shift is proportional to the average polarizability of the cluster. Fig. 2 shows an example of beam profiles measured for a nonpolar cluster (C_{60}) with and without an electric field in the deviator.

3.2. Rigid polar clusters

For polar clusters, the dominant contribution to the dipole in the electric field is due to the permanent dipole. For a rigid rotor with a fixed dipole μ_0, this contribution is equal to $\mu_0\langle\cos\theta\rangle$ where θ is the angle between the Z axis and the permanent dipole. For symmetric top molecules, the first order Stark effect [34]

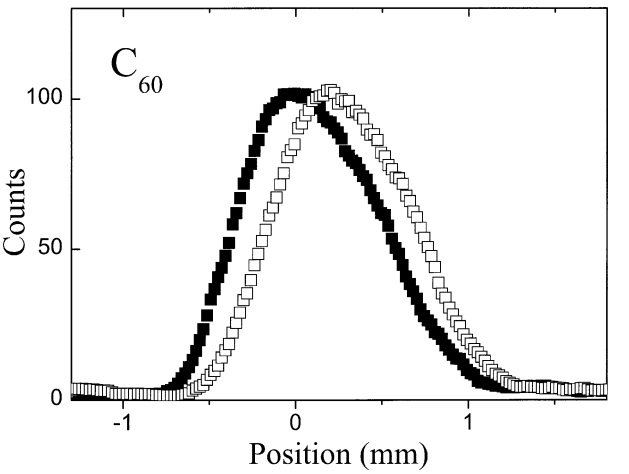

Figure 2. Beam profiles of C_{60} molecules: ■ experimental profile measured without electric field in the deviator (0 kV); □ experimental profile with $F = 1.5 \times 10^7$ Vm^{-1} in the deviator (25 kV).

is nonnull and there is a force proportional to the value of the electric field. For asymmetric top or linear molecules the average value of the cosine without electric field is zero at first order, and the force results of an interaction induced by the electric field between neighboring levels.

The Hamiltonien of the system in the electric field is:

$$H = H_{\text{rot}} - \vec{\mu} \cdot \vec{F} = H_{\text{rot}} - \mu_0 F_Z \cos(\theta) \tag{7}$$

For linear molecules, exact solutions for the Schrödinger equation with the above Hamiltonian can easily be obtained. For clusters at room temperature, levels with high J values are populated and the diagonalization of the above Hamiltonian would be a formidable task. For $\mu_0 F_Z/kT$ small, one can use a perturbative approach to compute the average value of $\cos(\theta)$ (see, for example, [35,36]).

For clusters, a classical calculation is a good alternative to the quantum mechanical approach. An exact calculation of the rotational motion in high electric field can be performed for symmetric top and linear molecules [37,38]. In a static field the Lagrangian of the system is (for a symmetric top rotor):

$$L = \frac{I_1}{2}\left(\dot{\theta}^2 + \dot{\varphi}^2 \sin^2\theta\right) + \frac{I_3}{2}(\dot{\psi} + \dot{\varphi}\cos\theta)^2 + \mu_0 F_Z \cos\theta \tag{8}$$

where θ, φ and ψ are the Euler angles, θ giving the inclination of the z axis of the symmetric top cluster from the direction Z of the electric field. The value of the two equal momenta of inertia of the cluster is I_1, the value of the third momentum of inertia is I_3. p_θ, p_φ and p_ψ are the conjugate momenta of θ, φ and ψ. p_φ and p_ψ are two constants of the motion. The average value of $\cos(\theta)$ is obtained from Eq. (8) as a function of p_φ, p_ψ and of the energy E of the cluster in the electric field. p_φ and p_ψ are invariant while the cluster enters the electric field. The value of E is deduced from the energy E_0 of the cluster before it enters the electric field using the adiabatic invariance of $\oint p_\theta \,\mathrm{d}\theta$ [39]. At a temperature T, the profile of deviation is given by [37]:

$$I(Z) = \frac{\iiiint \delta(Z - K\mu\nabla F\langle\cos(\theta)\rangle/(Mv^2)) \exp(-E_0/(kT)) \,\mathrm{d}p_\theta \,\mathrm{d}p_\varphi \,\mathrm{d}p_\psi \,\mathrm{d}\theta}{\iiiint \exp(-E_0/(kT)) \,\mathrm{d}p_\theta \,\mathrm{d}p_\varphi \,\mathrm{d}p_\psi \,\mathrm{d}\theta} \tag{9}$$

Fig. 3 shows an example of beam profiles measured for TiC_{60} ($\mu_0 = 8.1D$) with and without electric field in the deflector. The symbols correspond to the experimental profiles and the lines to profiles calculated using the classical method [37]. The value of $\langle\cos\theta\rangle$ and the average force depend on the rotational

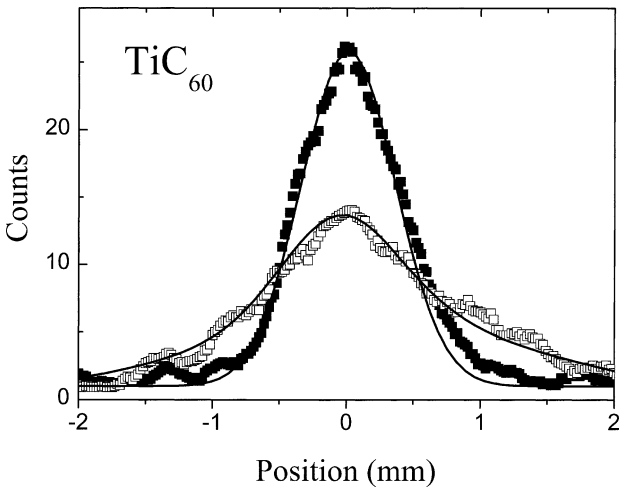

Figure 3. (a) Beam profiles of TiC_{60} molecules: ■ Experimental profile without electric field in the deviator (0 kV); □ experimental profiles with $F = 2.4 \times 10^6$ Vm^{-1} in the deviator (4 kV); (—) results of simulations at 0 kV and 4 kV for a dipole moment of $8.1D$, [37].

motion of the cluster. The electric field induces a broadening of the beam, which is well reproduced by the simulation.

Finally, as mentioned above, the effect of the induced dipole is for many systems, small when compared to the effect of the permanent dipole. It can be included in both quantum and classical calculations without any difficulty and it induces a global shift of the whole profile.

3.3. Nonrigid polar molecules

The rotational motion of a nonrigid rotor is no longer described by Eqs. (7) or (8); in particular coupling between the vibration and the rotation and potential parts of the Hamiltonian has to be taken into account. In the general case, the calculation of the projection of the dipole moment on the Z axis as a function of time is not possible. However, if the fluctuations of the particles are such that the distribution of dipoles in the electric field is given by a canonic distribution, a very simple formulation of the average value of the dipole in the electric field is available. Assuming a linear response, the average value of the dipole in the electric field is proportional to the fluctuations of the square of the dipole calculated with the unperturbed distributions (i.e., without electric field) and to the value of the electric field. The average value of the dipole is given by:

$$\langle \mu \rangle = \left[\alpha_{\text{avg}} + \frac{\langle \mu^2 \rangle_0}{3kT} \right] F_Z = \chi F_Z \tag{10}$$

where χ can be defined as the DC electric susceptibility of the cluster (the electronic polarizability is included in Eq. (10)). It is analog to the DC susceptibility of a paraelectric system. In this case, the deflected profiles are similar to the profiles obtained for a nonpolar cluster: there is a deviation without broadening. The polar contribution to Eq. (10) is in general much larger than the electronic contribution and is inversely proportional to the temperature. Examples of deflections measured for nonrigid clusters are given in Section 5. These results are similar to Stern and Gerlach's experiments performed on magnetic clusters with spins that are not locked to the cluster lattice [18–21]. For some model systems, the fluctuations of the cluster and of the dipole are easy to visualize [22,23], but a complete treatment and a justification of the use of Eq. (10) in the general case has not been developed yet (neither for electric, nor for magnetic dipole).

4. Atomic clusters

4.1. Metal clusters

In metal clusters, the electrons are delocalized and we expect that the polarizability follows in first approximation the law:

$$\alpha = (R + \delta)^3 = \left(N^{1/3} r_S + \delta\right)^3 \tag{11}$$

where δ is the electron spill-out and r_S the Wigner–Seitz radius. This means that the polarizability per atom of simple metal clusters is assumed to increase when the number of atoms decreases. The experimental evolution as a function of size was observed in various metals namely sodium, potassium, lithium, lithium-sodium, aluminum and recently nickel. We discuss firstly sodium clusters for which the measurements are the most numerous and complete.

4.1.1. *Sodium clusters*

The general properties of sodium clusters are well interpreted in the frame work of the Jellium model and sodium is the prototype of a simple metal cluster [1]. Fig. 4 shows measurements gathered from three independent experiments [11,28,40]. They cover a large size domain extending from the atom to 90 atoms. They show a global decrease with the size. However the results are in average above the approximate law (Eq. (11)) where $r_S = 2.12$ Å and $\delta = 0.69$ Å. Some dips are observed for shell closures $N = 8, 20$ but they are not very pronounced. Ab initio calculations [24,40–45] or more empirical methods [46] have been used to reproduce the experimental results. All the theoretical results agree with a global decrease as a function of size but they all underestimate the experimental values. This discrepancy between theory and experiment is usually explained by the influence of the temperature, the theoretical calculations being made at 0 K, while the cluster temperature is larger than 300 K, but not precisely known. Temperature influence on the polarizability has been recently calculated [25–27] but no conclusive comparison with experiment is available because precise measurements as a function of cluster temperature are lacking.

Except for this problem related to temperature effects, the above results are in agreement with a delocalization of valence electrons, even for very small sizes, as it is confirmed by ab initio calculations. The results on potassium clusters are less complete but they exhibit similar phenomena.

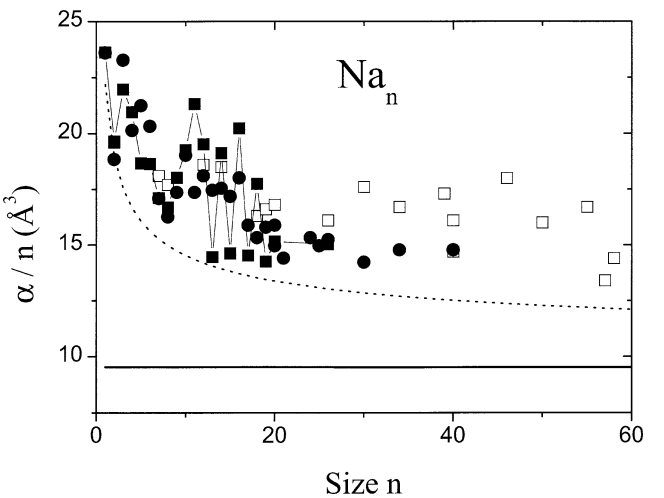

Figure 4. Static dipole polarizabilities per atom of sodium clusters plotted as a function of the number of atoms in the cluster: • data from [11]; ■ data from [40]; □ data from [28]. The dashed line represents the prediction from the classical metallic sphere (Eq. (11)) assuming a radius of 2.12 Å and an electron spill-out of 0.69 Å. The solid line corresponds to the bulk value. The precision in experimental measurements depends on the cluster size and experiments but it is typically ±10%.

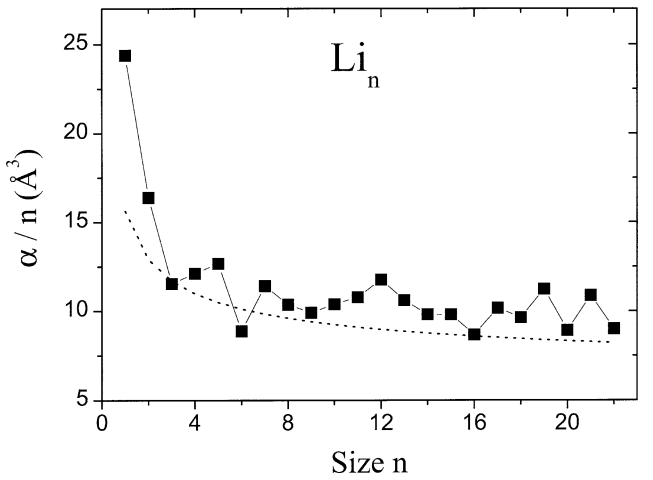

Figure 5. Static dipole polarizabilities per atom of lithium clusters plotted as a function of the number of atoms in the cluster [29]. The dashed line represents the prediction from the classical metallic sphere (Eq. (11)) assuming a radius of 1.75 Å and an electron spill-out of 0.75 Å. The precision in experimental measurements is ±10%.

4.1.2. *Lithium clusters*

The case of lithium clusters is very interesting. The atomic polarizability is abnormally large, very close to the sodium atomic value. On the other hand, the classical values for the corresponding metallic spheres are very different since the Wigner–Seitz radi are 1.75 Å and 2.12 Å for Li and Na, respectively.

The evolution of lithium clusters polarizability is shown in Fig. 5. In fact, this polarizability is very close to the finite metallic sphere for clusters larger than 3 or 4 atoms [29,40]. The abnormal value for the lithium atom is due to the diffuse character of the valence electron which occupies about the same volume as in the sodium atom. In clusters, the valence electrons are delocalized in a volume that principally depend on internuclear distances. Even for very small sizes, these distances are close to the bulk values, because they are mainly related to the ion sizes. This evolution of the polarizability in lithium illustrates the delocalization of the valence electrons in alkali clusters, from 3 or 4 atoms. This also shows that the red-shift of the dipole resonance of lithium clusters, as compared to the Mie theory is not related to static polarizability but to an effective mass effect [29], which is due to nonlocal pseudopotential and affects the dynamic response [47].

The electric polarizability of mixed sodium–lithium clusters have also been measured for small sizes [12]. They decrease continuously from pure sodium, to pure lithium clusters as a function of the lithium content. They are in good agreement with ab initio calculations.

4.1.3. *Other metals*

The measurements of electric polarizability of other metal clusters are quite scarce. To our knowledge, only aluminum and nickel clusters have been studied. These measurements are difficult because in most metals the polarizability per atom is much smaller than in alkali metals. In aluminum clusters [13], where results are available for up to 60 atoms, the behavior as a function of size is very different from that of alkali metals (Fig. 6). The polarizability increases from the atom to the dimer and is below the empiric law (Eq. (11)) or Thomas–Fermi approximation [1,13,48] in the size range $15 < N < 40$. This is generally interpreted by the bonding change in aluminum as a function of the size, the s electron of aluminum (atomic structure $s^2 p$) being only partially delocalized for small sizes [49].

The results recently obtained for nickel clusters [30] are very interesting but much more difficult to interpret. They are close to the empiric law (Eq. (11)) in absolute values, but they do not follow the slow decrease as a function of size and tend rather to slightly increase (Fig. 6). Moreover, anomalous high values are obtained for some sizes Ni_{21}, Ni_{22} and Ni_{49-54}. These sizes are expected to correspond to icosahedron or polyicosahedron with 'missing' atoms. This kind of measurement is crucial for the determination of nickel cluster structure but quite hard theoretical calculations are necessary to interpret them, the ab initio calculations in transition metal clusters remaining a difficult challenge.

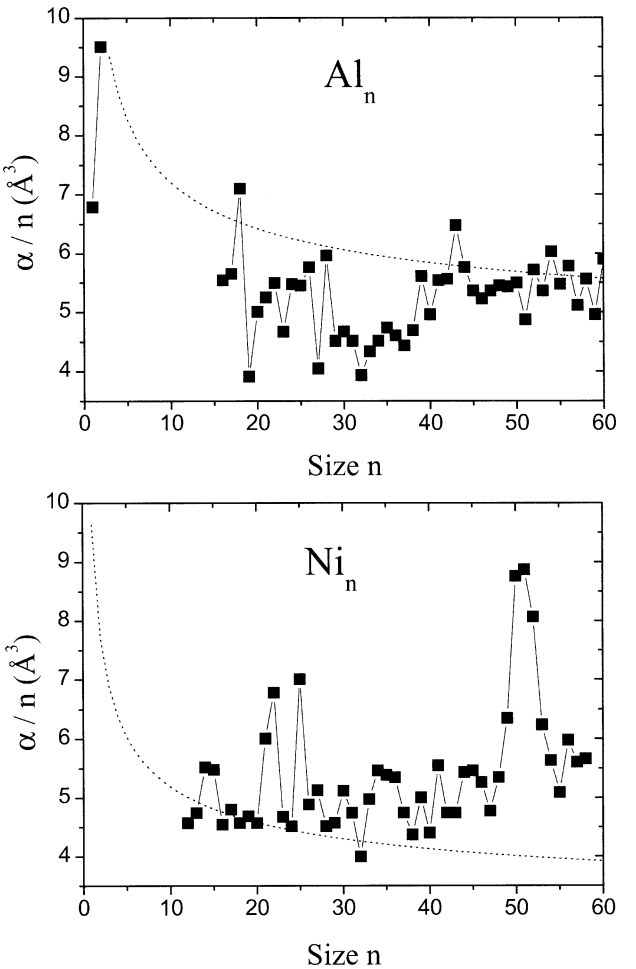

Figure 6. Static dipole polarizabilities per atom of aluminum [13] and nickel [30] clusters plotted as a function of the number of atoms in the cluster. The dashed lines represent the prediction from the classical metallic sphere assuming a radius of 1.58 Å and 1.39 Å, an electron spill-out of 0.76 Å and 0.74 Å for aluminum and nickel, respectively. The precision in experimental measurements is of the order of ±10% for aluminum and ±20% for nickel.

4.2. Covalent clusters

In these systems (carbon, silicon, germanium) the electrons are not delocalized and the bonding has a covalent character. The comparison with the bulk is usually realized through the Clausius–Mossotti relation:

$$\alpha = \frac{\varepsilon - 1}{\varepsilon + 2} r_S^3 N^3 \tag{12}$$

where ε is the static dielectric function, and r_S the Wigner–Seitz radius.

The available results concern silicon clusters, other semiconductor clusters, and fullerenes.

4.2.1. *Silicon and other semiconductor clusters*

The polarizability of silicon clusters have been measured by beam deviation in the size range $10 < N < 120$ [14]. They are plotted in Fig. 7. The experimental values for α are below the bulk value $\alpha_{\text{bulk}} = 3.71$ Å^3 deduced from relation (12) and strong variations from size to size are observed with high values for $N = 10, 17, 23, 29$.

The comparison between theory and experiment is quite puzzling for silicon. The polarizability is calculated by higher-order finite-difference method with nonlocal pseudopotentials [50] or first principles

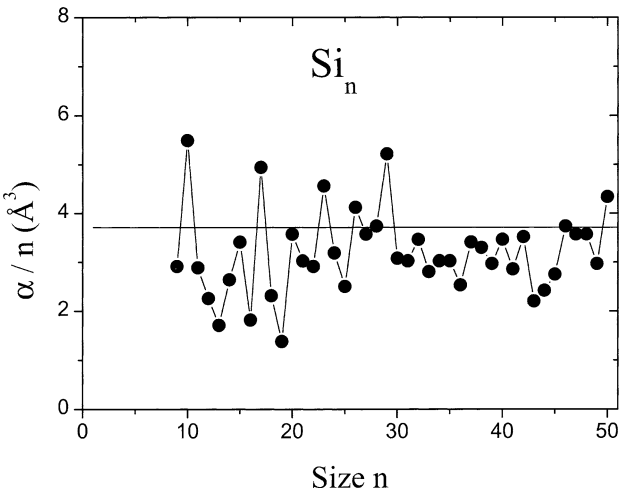

Figure 7. Polarizabilities per atom of SiN clusters [14]. The solid line corresponds to the bulk value. The precision in experimental measurements depends on the cluster size but it is typically ±25%.

density-functional-based method [51,52]. The available results extend from one atom to 28 atoms. The obtained polarizabilities are all above the bulk value, contrary to experimental results. They do not reproduced relative size variations. The theoretical results are interpreted by the existence of dangling bonds in small silicon clusters which results in averaged coordination numbers larger than 4. This is sometimes called the metallic-like nature of small silicon clusters [50] and may explain the fact that calculated values are above the bulk one. Values are less regular than in simple metals because the averaged coordination number depends on size and for a given size on the structure. It is known that several isomers may coexist in a molecular beam [53] and this renders more difficult the comparison with the experiment. Nevertheless, experimental and theoretical trends are not in agreement. The precision in the experimental values is not very high, typically ±20%. We believe that this precision must be improved before a definitive conclusion can be made. The question of the electric polarizability in small silicon clusters remains open, as well as the electronic structure of these clusters.

The polarizability of other semi-conductor clusters like $Ga_N As_M$ (N close to M) has been measured as a function of $N + M$ in the size range $5 < N + M < 30$ [14]. The results illustrate the importance of donor-like or acceptor-like defect states in the band gap. For odd values of the total number of atoms $N + M$, defect states exist in the band gap and lead to high values of the polarizability, while for even values of $N + M$, there are no defect states and the polarizability is much smaller. This results in a nice odd-even alternation in the polarizability values as a function of the cluster size. $Ge_N Te_M$ clusters have also been studied [14]. In this case, a strong temperature dependence is observed. This may be related to the ferroelectric character of GeTe bulk. It would be very interesting to study this system more systematically as a function of temperature to investigate the influence of the paraelectric-ferroelectric transition and of the melting point in these small systems.

4.2.2. *Fullerenes*

The experimental polarizability of small carbon clusters is not available. Therefore we will discuss only the case of C_{60} and C_{70} fullerenes for which measurements have been recently performed [15–17]. For these new systems, the Clausius Mossoti relation cannot be used to deduce the polarizability per atom from the dielectric constant of graphite or diamond, because the bonding and the structure are completely different (new forms of carbon). However the Clausius Mossotti relation may be used to deduce the polarizability of C_{60} and C_{70} from fullerites (C_{60} and C_{70} bulk).

The measured values of static polarizability for C_{60} and C_{70} are 76.5 ± 8 Å^3 and 102 ± 14 Å^3 respectively [15,16]. In Table 1, these values are compared to other measurements deduced from the bulk (C_{60} and

Table 1. Experimental and theoretical results for the averaged static polarizability of C_{60} and C_{70}. For C_{60} and C_{70} films, the polarizability value is extracted from the experimental dielectric function by using the Clausius–Mossotti relation.

Method	$\alpha(C_{60})$ (Å^3)	$\alpha(C_{70})$ (Å^3)	$\alpha(C_{70})/\alpha(C_{60})$
Experiment			
Gas phase			
Molecular Beam Deviation [16]	76.5 ± 8	102 ± 14	1.33 ± 0.03
C_{60} and C_{70} films			
Optical measurements: ellipsometry and reflection/transmission [69][1]	79.0	97.0	1.23
Electron Energy-Loss Spectroscopy [70]	83.0	103.5	1.25
Theory			
Iterative coupled Hartree–Fock (STO-3G basis set) [71]	45.6	57.0	1.25
Pariser–Parr–Pople Hamiltonian [72]	49.4	63.8	1.29
Atom Monopole–Dipole Interaction [73]	60.8	73.8	1.21
Semi empirical calculation (MNDO/PM3) [74]	63.9	79.0	1.24
Ab initio SCF (6-31++G basis set) [54]	75.1	89.8	1.20
Tight binding – Linear response [16]	77.0	91.6	1.19
Bond polarizability model [75]	89.2	109.2	1.22
Valence effective Hamiltonian [76]	154.0	214.3	1.39
Model			
Additivity model			1.17
Conducting shell model			1.22

[1] In the Clausius–Mossotti relation, we used a lattice constant $a = 14.17$ Å for C_{60} and $a = 15.01$ Å for C_{70}.

C_{70} films) and to theoretical calculations including ab initio methods, tight binding and rough models. In Table 1, we limit the comparison to calculations performed for both C_{60} and C_{70}. The agreement between values obtained by beam deviation and from C_{60} and C_{70} films is very good. The theoretical values show large variations from 45 to 154 Å^3 for C_{60} and 57 to 214.3 Å^3 for C_{70}. The best theoretical results are obtained by ab initio methods [54] and tight binding linear response [16]. The rough model of conducting shell taking into account the thickness of the electronic cloud also leads to good results, 77 and 94 Å^3 for C_{60} and C_{70} respectively [16].

Due to the difficulty of absolute calibration, the ratio $\alpha_{C_{60}}/\alpha_{C_{70}}$ is known with a better precision than $\alpha_{C_{60}}$ and $\alpha_{C_{70}}$ separately (Table 1). The experimental value is larger than the simple additivity of atomic contribution which gives 1.17 $(7/6)$ for this ratio. This is expected but the experimental value of 1.33 is also larger than the best theoretical predictions (typically 1.2–1.22). On the experimental side, the isomerization of C_{70} and the finite temperature (300 K) of the experiment may be evoked to explain these differences. Further experimental and theoretical investigations including larger and smaller fullerenes are necessary to permit a conclusion. Nevertheless, in fullerenes, due to the cage structure, the polarizability per atom tends to increase as a function of size. A similar behavior is expected for carbon chains. This is very different from metal clusters where the electron delocalization tends to induce compact structures having polarizabilities per atom that decrease as the cluster size increases (the relative contribution of the spill-out decreasing with size).

Finally the optical polarizability of C_{60} has been measured by beam deviation with a light standing wave at 1064 nm [17]. The obtained value ($\alpha_{opt} = 79 \pm 4$ Å^3) is slightly higher than the static one ($\alpha_{sta} = 76.5 \pm 8$ Å^3), in agreement with most recent ab initio calculations [55] giving 76.4 and 75.1 Å^3, respectively. Measurements at other wavelengths, typically 532 nm would be very interesting to have a good picture of the frequency evolution of the C_{60} polarizability.

5. Mixed clusters

First experiments on mixed clusters [14] were performed on 3–5 and 2–6 semiconductor clusters. These experiments have already been discussed in the atomic clusters section because they are really characteristic of semiconductor behavior and the results are strongly connected to silicon results.

5.1. Metal fullerene clusters

In metal–C_{60} molecules, a charge transfer from the metal atom to the fullerene induces a strong permanent electric dipole. This charge transfer was first observed in photoelectron spectroscopy experiments [56, 57] and plays a key role in the electrical conductivity and superconductivity properties of fullerites doped by alkali metal atoms [58,59]. The first molecular deflection experiments were performed in our group two years ago [22,60]. Fig. 8 shows experimental profiles measured with and without an electric field for KC_{60} at room temperature. A strong deviation without broadening is observed. This is a text book example of nonrigid cluster. At room temperature, the alkali atom, and then the direction of the electric dipole moment, can move freely on the surface of the cage. Without the electric field, the average value of the dipole is zero. In a static electric field, the dipole is statistically oriented toward the direction of the electric field

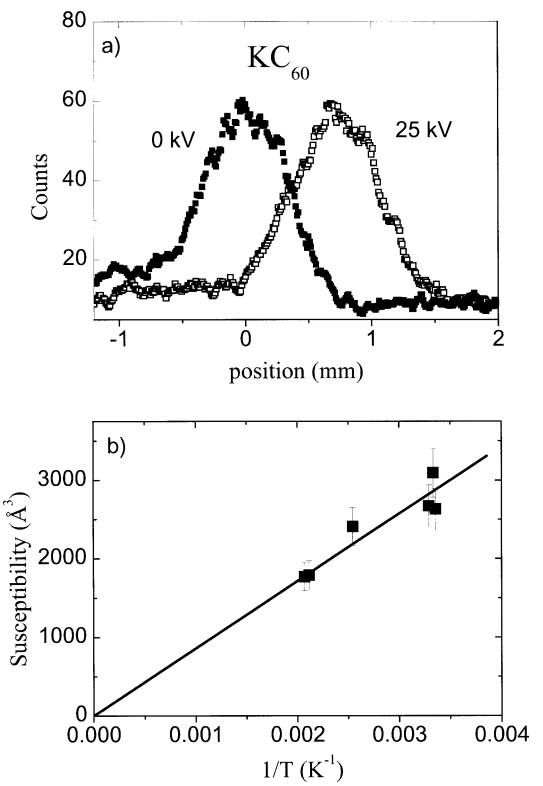

Figure 8. (a) Experimental beam profiles of KC_{60} molecules, with and without electric field in the deflector (0 kV and 25 kV); (b) Susceptibility of KC_{60} plotted as a function of the inverse of the temperature. The line corresponds to a linear fit of the data. The temperature of the nozzle has been varied from 300 K to 483 K [22].

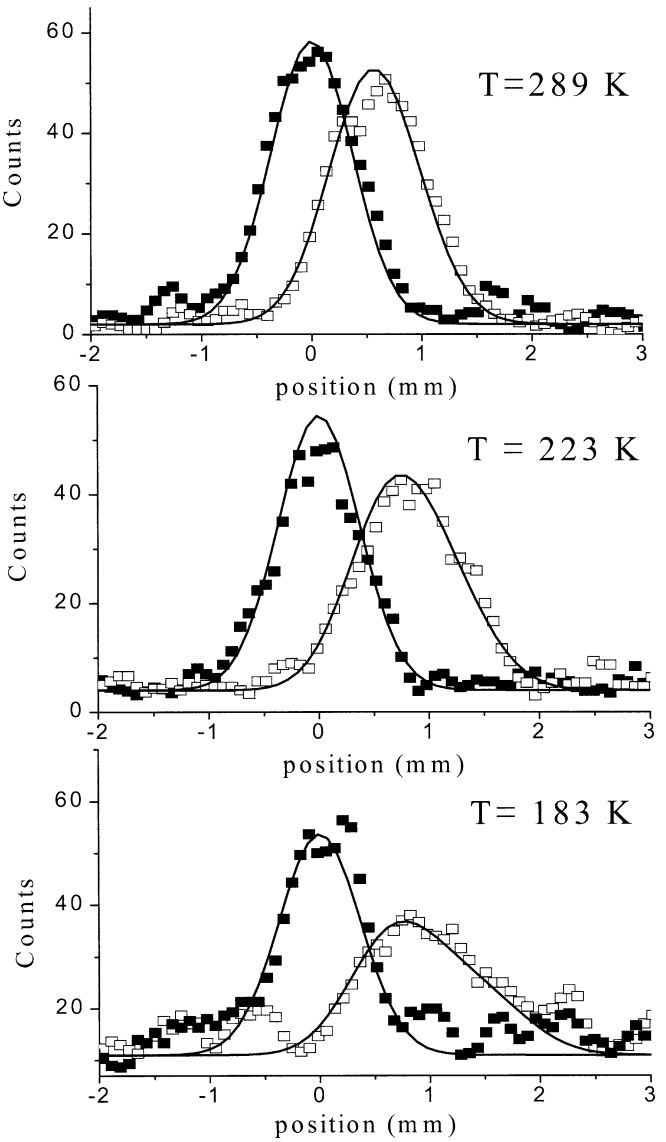

Figure 9. Beam profiles of RbC_{60} molecules measured at 3 different temperatures: ■ experimental profiles without deviation ($V = 0$ kV); □ experimental profiles with $V = 24$ kV across the deviator; (—) results of simulation for $V = 0$ kV and $V = 24$ kV for a dipole moment of $20.6D$ [23].

and its average value is given by Eq. (10). Fig. 8(b) shows that above room temperature the experimental susceptibility is inversely proportional to the temperature as predicted by Eq. (10).

Fig. 9 shows experimental profiles measured below room temperature. As the temperature decreases, the hopping or fluctuation frequency of the alkali atom decreases and the value of the average dipole does not follow the Langevin formula (Eq. (10)). The deviation is not the same for all the clusters: all the clusters do not have the same average dipole. In this particular case of an atom on C_{60}, the evolution of the polarizability with temperature is perfectly reproduced with a very simple statistical model of relaxation which takes into account the rotational motion of the molecule [23]. This model allows a precise determination of the dipole of the cluster at equilibrium and of the barrier of energy to hop from one equilibrium site to another. Permanent dipole moments measured for LiC_{60}, NaC_{60}, KC_{60}, and CsC_{60} [61] are listed in Table 2. The dipole moment increases with the size of the alkali atom, from $12.4D$ for LiC_{60} to $21.5D$ for CsC_{60}. This

Table 2. Experimental permanent dipole moment obtained from deviation measurements for alkali metal-C_{60} clusters [61].

	LiC_{60}	NaC_{60}	KC_{60}	RbC_{60}	CsC_{60}
$\mu_{exp}(D)$	12.4 ± 2.0	16.3 ± 1.6	21.5 ± 2.2	20.6 ± 2.1	21.5 ± 2.2

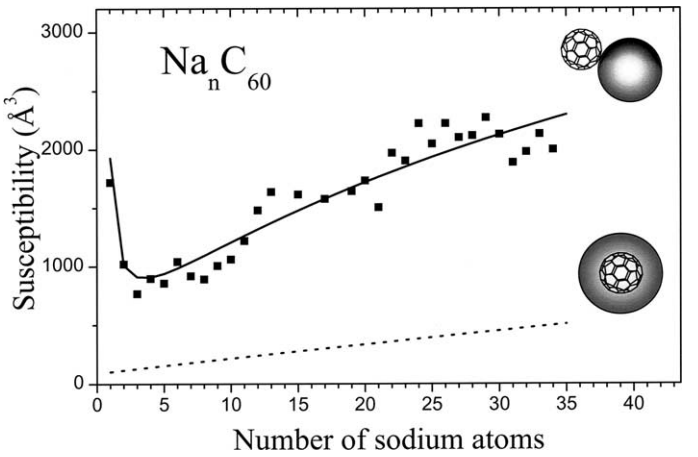

Figure 10. Susceptibility of $Na_N C_{60}$ clusters as a function of the number of sodium atoms. The dark squares correspond to experimental values [62]. The full line corresponds to values calculated assuming that the sodium atoms form a metal shell around the fullerene. The dashed line corresponds to the values calculated assuming the formation of a metal droplet on the surface of the fullerene (see [62]).

evolution is mainly due to the decrease in the ionization potential of the alkali atom and is well reproduced by a simple analytical polarizable-ion model [61].

The same measurements were extended to clusters with several alkali atoms ($Na_n C_{60}$ clusters) [62]. The results are given in Fig. 10 for $n = 1$ to 34. Comparison of these results with two simple models shows that the sodium does not wet the C_{60} but clusters on its surface to form a small metal droplet. This result is different from the interpretation of mass spectrometry [63], or photoelectron spectroscopy experiments performed on ionic systems [57]. This may reflect that a change in the charge state can drive a complete reorganization of the cluster geometry.

5.2. Alkali halide clusters

The very first electric beam deviation experiments with polar molecules were performed in 1927 [64] on alkali halide molecules which have a large permanent electric dipole due to the ionic nature of the bond. Alkali halide clusters are ionic and tend to form small cubic nanocrystals with a lattice structure similar to the NaCl structure. For clusters, the first deviation experiments were performed in 2000 on cesium bromide clusters with one excess electron [65]. The experimental results are plotted in Fig. 11; they strongly depend on the cluster size. However, no direct correlation between deflection results and the ionization potential pattern or the families defined in previous experiments [66–68] is observed.

A study of the beam deflection as a function of the temperature for $Cs_{18}Br_{17}$ shows that its susceptibility follows Eq. (10) with a main contribution due to its permanent dipole. Using Eq. (10), experimental results are in qualitative agreement with the permanent dipoles expected for structures that were previously determined for sodium fluoride clusters [67,68]. For example, the structure of $Na_{18}F_{17}$ is a $4 \times 3 \times 3$ parallelepiped with a F center. To first approximation, this cluster is made of an even number of layers alternatively positively and negatively charged leading to a large permanent dipole. In the same way, a similar dipole is expected for $Cs_{30}Br_{29}$ and a dipole two times smaller for Cs_9Br_8. The large values observed for $Cs_{14}Br_{13}$ may be due to the localization of the excess electron on a corner [68]. Despite the simplicity of ionic bonding, the interpretation of the results obtained for cesium bromide clusters is not complete and further experimental and theoretical studies are needed.

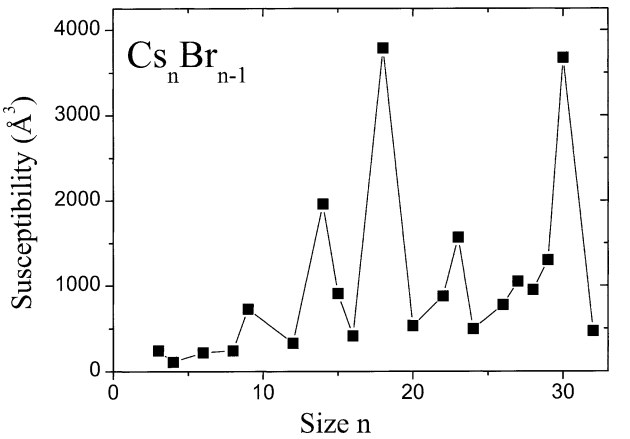

Figure 11. Susceptibility of Cs_nBr_{n-1} clusters [65]. Data are missing for certain sizes. The line has been plotted to guide the eyes. The precision in the experimental measurements is ±10%.

6. Conclusions

The measurement of electric polarizability of small atomic clusters is a powerful way to probe their electronic structure and the type of bonding between atoms, including metal bonding (electron delocalization), covalent bonding, ionic bonding, existence of states inside the gap for semiconductors, etc. Comparison between precise measurements and high level theoretical calculations is the key for a deep understanding of these electronic properties. This comparison is well achieved in alkali clusters where the main features are well understood and the next step for these systems would be an extended study of the temperature dependence. For other metal clusters, the experimental results are not very numerous and the theoretical calculations are quite hard. Nevertheless the different behaviour between alkali and other metal clusters (Al, Ni) is striking and this should probably require more attention in the future. For example, correlation in transition metal clusters between strong size effects in electric polarizabilities and chemical reactivity is probably very interesting.

For covalent and semiconductor clusters, the polarizability is also an important and key property. In silicon, the structure of small clusters is very complicated, with a large number of isomers. If the polarizability measurements do not bring new insight, they need probably to be improved in parallel to progresses in theory. In Ga_NAs_M clusters, the high value of the electric polarizability for some sizes has been shown to be a clear signature of defect states inside the gap.

Fullerenes are prototypes to study the relation between structure and electric polarizability, and the recently obtained results for C_{60} and C_{70} are a first step in this direction. For the future, measurements on larger or smaller fullerenes are necessary to have a complete description of these cage molecules. Moreover, at least for C_{60}, it becomes now possible to describe the behavior of the electric polarizability as a function of the frequency up to the optical regime.

For these atomic clusters, measurements of the polarizability as a function of the temperature could open a new field, for example liquid–solid transitions for most systems or paraelectric–ferroelectric transitions in some specific cases. For liquid–solid transitions the polarizability may be a direct manifestation of the evolution of interatomic distance during such a transition.

In mixed clusters, using beam deviation techniques, it becomes possible to measure dipole moment through broadening of the beam (rigid molecules), or dipole susceptibility (nonrigid molecules). This is clearly illustrated for the metal-fullerene system where charge transfer as well as metal segregation have been measured. This technique, developed for studying clusters, may be used for any complex molecule where the electric dipole is very often a key parameter directly related to the geometric arrangement and conformation. Biologic molecules in the gas phase are good candidates. For example, polypeptides may form helices with large electric dipole or more compact structures with small dipole. The beam

deviation technique may give a signature of different isomers, opening the road for a two-dimensional mass spectrometry: the mass number being obtained by time of flight and the dipole by beam deviation.

Acknowledgements. Several scientists have contributed to the present project. F.W. Dalby and B. Vezin participated to the first experiments. C. Guet, F. Chandezon, B. Huber, C. Ristori and J.C. Rocco from CEA Grenoble were associated with us in building the apparatus and participated in the measurements on atomic clusters. A.R. Allouche, M. Aubert-Frécon and J. Lermé were involved in the theoretical part of our project. F. Spiegelman contributed also by helpful discussions and was involved in alkali halide calculations. The project benefits also of a strong and essential technical assistance from M. Barbaire, C. Clavier and J. Maurelli.

References

[1] W.A. deHeer, Rev. Mod. Phys. 65 (1993) 611.
[2] J. Blanc, V. Bonacic-Koutecky, M. Broyer, J. Chevaleyre, P. Dugourd, J. Koutecky, C. Scheuch, J.P. Wolf, L. Wöste, J. Chem. Phys. 96 (1992) 1793.
[3] J. Ho, K.M. Ervin, W.C. Lineberger, J. Chem. Phys. 93 (1990) 6987.
[4] O. Cheshnovsky, K.J. Taylor, J. Conceicao, R.E. Smalley, Phys. Rev. Lett. 64 (1990) 1785.
[5] J.C. Pinare, B. Baguenard, C. Bordas, Phys. Rev. Lett. 81 (1998) 2225.
[6] C. Bréchignac, P. Cahuzac, F. Carlier, M.D. Frutos, J. Leygnier, J. Chem. Phys. 93 (1990) 7449.
[7] R. Antoine, P. Dugourd, D. Rayane, E. Benichou, M. Broyer, J. Chem. Phys. 107 (1997) 2664.
[8] M.F. Jarrold, J. Phys. Chem. 99 (1995) 11.
[9] T.M. Miller, B. Bederson, Adv. At. Mol. Phys. 13 (1977) 1.
[10] K.D. Bonin, V.V. Kresin, Electric-Dipole Polarizabilities of Atoms, Molecules and Clusters, World Scientific, Singapore, 1997.
[11] W.D. Knight, K. Clememger, W.A. deHeer, W.A. Saunders, Phys. Rev. B 31 (1985) 2539.
[12] R. Antoine, D. Rayane, A.R. Allouche, M. Aubert-Frécon, E. Benichou, F.W. Dalby, P. Dugourd, M. Broyer, C. Guet, J. Chem. Phys. 110 (1999) 5568.
[13] W.A. deHeer, P. Milani, A. Chatelain, Phys. Rev. Lett. 63 (1989) 2834.
[14] R. Schäfer, S. Schlecht, J. Woenckhaus, J.A. Becker, Phys. Rev. Lett. 76 (1996) 471.
[15] R. Antoine, P. Dugourd, D. Rayane, E. Benichou, M. Broyer, F. Chandezon, C. Guet, J. Chem. Phys. 110 (1999) 9771.
[16] I. Compagnon, R. Antoine, M. Broyer, P. Dugourd, J. Lermé, D. Rayane, Phys. Rev. A 64 (2001) 025201.
[17] A. Ballard, K. Bonin, J. Louderback, J. Chem. Phys. 113 (2000) 5732.
[18] W.A. deHeer, P. Milani, A. Chatelain, Phys. Rev. Lett. 65 (1990) 488.
[19] J.P. Bucher, D.C. Douglass, L.A. Bloomfield, Phys. Rev. Lett. 66 (1991) 3052.
[20] D.C. Douglass, J.P. Bucher, L.A. Bloomfield, Phys. Rev. Lett. 68 (1992) 1774.
[21] I.M.L. Billas, J.A. Becker, A. Châtelain, W.A. deHeer, Phys. Rev. Lett. 71 (1993) 4067.
[22] D. Rayane, R. Antoine, P. Dugourd, E. Benichou, A.R. Allouche, M. Aubert-Frécon, M. Broyer, Phys. Rev. Lett. 84 (2000) 1962.
[23] P. Dugourd, R. Antoine, D. Rayane, E. Benichou, M. Broyer, Phys. Rev. A 62 (2000) 011201 (R).
[24] S. Kümmel, T. Berkus, P.G. Reinhard, M. Brack, Eur. Phys. J. D 11 (2000) 239.
[25] S. Kümmel, J. Akola, M. Manninen, Phys. Rev. Lett. 84 (2000) 3827.
[26] L. Kronik, I. Vasiliev, J.R. Chelikowsky, Phys. Rev. B 62 (2000) 9992.
[27] S.A. Blundell, C. Guet, R.R. Zope, Phys. Rev. Lett. 84 (2000) 4826.
[28] G. Tikhonov, V. Kasperovich, K. Wong, V.V. Kresin, Phys. Rev. A 64 (2001) 063202.
[29] E. Benichou, R. Antoine, D. Rayane, B. Vezin, F.W. Dalby, P. Dugourd, M. Broyer, C. Ristori, F. Chandezon, B.A. Huber, J.C. Rocco, S.A. Blundell, C. Guet, Phys. Rev. A 59 (1999) R1.
[30] M.B. Knickelbein, J. Chem. Phys. 115 (2001) 5957.
[31] U. Hohm, Vacuum 58 (2000) 117.
[32] R.W. Molof, T.M. Miller, H.L. Schwartz, B. Bederson, J.T. Park, J. Chem. Phys. 61 (1974) 1816.
[33] E. Benichou, A.R. Allouche, R. Antoine, M. Aubert-Frécon, M. Bourgoin, M. Broyer, P. Dugourd, G. Hadinger, D. Rayane, Eur. Phys. J. D 10 (2000) 233.
[34] C.H. Townes, A.L. Shawlow, Microwave Spectroscopy, McGraw-Hill, New York, 1955.
[35] H. Scheffers, Phys. Z. 41 (1940) 89.
[36] I. Compagnon, F.C. Hagemeister, R. Antoine, D. Rayane, M. Broyer, P. Dugourd, R.R. Hudgins, M.F. Jarrold, J. Am. Chem. Soc. 123 (2001) 8440.
[37] P. Dugourd, I. Compagnon, F. Lepine, R. Antoine, D. Rayane, M. Broyer, Chem. Phys. Lett. 336 (2001) 511.
[38] H. Goldstein, Classical Mechanics, Addison-Wesley, Reading, MA, 1980.

[39] L. Landau, E. Lifchitz, Physique Théorique, Tome 1, Mécanique, Mir, Moscou, 1966.
[40] D. Rayane, A.R. Allouche, E. Benichou, R. Antoine, M. Aubert-Frécon, P. Dugourd, M. Broyer, C. Ristori, F. Chandezon, B.A. Huber, C. Guet, Eur. Phys. J. D 9 (1999) 243.
[41] I. Moullet, J. Luriaas, M.F. Reuse, J. Buttet, Phys. Rev. Lett. 65 (1990) 476.
[42] J.M. Pacheco, J.L. Martins, J. Chem. Phys. 106 (1997) 6039.
[43] L. Kronik, I. Vasiliev, M. Jain, J.R. Chelikowsky, J. Chem. Phys. 115 (2001) 4322.
[44] P. Calaminici, K. Jug, A.M. Köster, J. Chem. Phys. 111 (1999) 4613.
[45] S.J.A.V. Gisbergen, J.M. Pacheco, E.J. Baerends, Phys. Rev. A 63 (2001) 063201.
[46] V.V. Kresin, Physics Reports 220 (1992) 1.
[47] S.A. Blundell, C. Guet, Zeit. Phys. D 33 (1995) 153.
[48] V.V. Kresin, Phys. Rep. 220 (1990) 1.
[49] E. Cottancin, M. Pellarin, J. Lermé, B. Baguenard, B. Palpant, J.L. Vialle, M. Broyer, J. Chem. Phys. 107 (1997) 757.
[50] I. Vasiliev, J.R. Chelikowsky, Phys. Rev. Lett. 78 (1997) 4805.
[51] K. Jackson, M. Pederson, C.-Z. Wang, K.-M. Ho, Phys. Rev. A 59 (1999) 3685.
[52] K. Deng, J. Yang, C.T. Chan, Phys. Rev. A 61 (2000) 025201.
[53] A.A. Shvartsburg, R.R. Hudgins, P. Dugourd, M.F. Jarrold, Chem. Soc. Rev. 30 (2001) 26.
[54] D. Jonsson, P. Norman, K. Ruud, H. Agren, T. Helgaker, J. Chem. Phys. 109 (1998) 572.
[55] K. Ruud, D. Jonsson, P.R. Taylor, J. Chem. Phys. 114 (2001) 4331.
[56] L.-S. Wang, O. Cheshnovsky, R.E. Smalley, J.P. Carpenter, S.J. Hwu, J. Chem. Phys. 96 (1992) 4028.
[57] B. Palpant, A. Otake, F. Hayakawa, Y. Negishi, G.H. Lee, A. Nakajima, K. Kaya, Phys. Rev. B 60 (1999) 4509.
[58] R.C. Haddon, A.F. Hebard, M.J. Rosseinski, D.W. Murphy, S.J. Duclos, K.B. Lyons, B. Miller, J.M. Rosamilia, R.M. Fleming, A.R. Kortan, S.H. Glarum, A.V. Makhija, A.J. Muller, R.H. Eick, S.M. Zahurak, R. Tycko, G. Daddagh, F.A. Thiel, Nature (London) 350 (1991) 320.
[59] D.W. Murphy, M.J. Rosseinsky, R.M. Fleming, R. Tycko, A.P. Ramirez, R.C. Haddon, T. Siegrist, G. Dabbagh, J.C. Tully, R.E. Walstedt, J. Phys. Chem. Solids 53 (1992) 1321.
[60] I. Compagnon, R. Antoine, D. Rayane, P. Dugourd, M. Broyer, Eur. Phys. J. D 16 (2001) 365.
[61] R. Antoine, D. Rayane, P. Dugourd, E. Benichou, M. Broyer, Eur. Phys. J. D 12 (2000) 147.
[62] P. Dugourd, R. Antoine, D. Rayane, I. Compagnon, M. Broyer, J. Chem. Phys. 114 (2001) 1970.
[63] U. Zimmermann, N. Malinowski, A. Burkhardt, T.P. Martin, Carbon 33 (1995) 995.
[64] V.E. Wrede, Z. Phys. 44 (1927) 261.
[65] D. Rayane, R. Antoine, P. Dugourd, M. Broyer, J. Chem. Phys. 113 (2000) 4501.
[66] E.C. Honea, M.L. Homer, P. Labastie, R.L. Whetten, Phys. Rev. Lett. 63 (1989) 394.
[67] G. Durand, F. Spiegelmann, P. Poncharal, P. Labastie, J.M. L'Hermite, M. Sence, J. Chem. Phys. 110 (1999) 7884.
[68] G. Durand, J. Giraud-Girard, D. Maynau, F. Spielgelmann, F. Calvo, J. Chem. Phys. 110 (1999) 7871.
[69] S.-L. Ren, K.-A. Wang, P. Zhou, Y. Wang, A.M. Rao, M.S. Meier, J.P. Selegue, P.C. Eklund, Appl. Phys. Lett. 61 (1992) 124.
[70] E. Sohmen, J. Fink, W. Krätschmer, Z. Phys. B 86 (1992) 87.
[71] J. Baker, P.W. Fowler, P. Lazzeretti, M. Malagoli, R. Zanasi, Chem. Phys. Lett. 184 (1991) 182.
[72] F. Willaime, L.M. Falicov, J. Chem. Phys. 98 (1993) 6369.
[73] B. Shanker, J. Applequist, J. Phys. Chem. 98 (1994) 6486.
[74] N. Matsuzawa, D.A. Dixon, J. Phys. Chem. 96 (1992) 6241.
[75] S. Guha, J. Menéndez, J.B. Page, G.B. Adams, Phys. Rev. B 53 (1996) 13 106.
[76] Z. Shuai, J.L. Brédas, Phys. Rev. B 46 (1992) 16135.